



## Experimental Study Using the Passive Solar Chimney for Evaporative Cooling With PCM and CFM as a Thermal Energy Storage

Talib K. Murtadha\*      Hussien M. Salih\*\*      Ali D. Salman\*\*\*

\*Department of Mechanical Engineering/ University of Technology

\*\* , \*\*\*Department of Electro- Mechanical Engineering/ University of Technology

\*Email: [talib\\_km@yahoo.com](mailto:talib_km@yahoo.com)

\*\* Email: [husein\\_maj@yahoo.com](mailto:husein_maj@yahoo.com)

\*\*\* Email: [aligaphory@yahoo.com](mailto:aligaphory@yahoo.com)

(Received 11 January 2016; accepted 17 April 2016)

### Abstract

In this work, a test room was built in Baghdad city, with  $(2*1.5*1.5)$  m<sup>3</sup> in dimensions, while the solar chimneys (SC) were designed with aspect ratio (ar) bigger than 12. Test room was supplied by many solar collectors; vertical single side of air pass with ar equals 25, and tilted 45° double side of air passes with ar equals 50 for each pass, both collectors consist of flat thermal energy storage box collector (TESB) that covered by transparent clear acrylic sheet, third type of collector is array of evacuated tubular collectors with thermosyphon in 45° instilled in the bottom of TESB of vertical SC. The TESB was made from metallic iron sheets as a shell and fuelled by paraffin wax as phase change material (PCM). The PCM supported by copper foam matrix (CFM) to enhance thermal conductivity of wax. When heat is released from TESB to the air, a buoyancy force will be generated in chimney gaps. Then a difference in pressure between inside and outside test room leads to induce the air flow to test room through wet corrugated cellulose pad, where evaporative cooling (EC) occurs. Results of experimental work, that achieved in June, for 12 to 24 hour in the test day, refer to effectiveness using EC to decrease the room temperature comparing. The system reduces test room temperature of up to 8.5~9.2 °C in 11:00 am to 3:00 pm and at highest effectiveness of EC, while minimum reduces in temperature of up to 3.5 °C in 8:00pm to 3:00 am. Also, the results showed the affectivity to using the TESB, during the night time for ventilation and EC, with lower effectiveness than from day time. The range of EC effectiveness equals 30.5-37.5 with a natural vent, while The maximum air change per hour (ACH) equals (3.8-6.187), and the maximum mass flow rate is equal to (36.651 kg.hr<sup>-1</sup>) at experimental evaluation of the system's discharge coefficient value 0.371.

**Key words:** Solar chimney , evacuated tubular collector, phase change material, copper foam matrix.

### 1. Introduction

The energy consumed for space air conditioning, for heating or cooling and ventilation, depends on the latitude and altitude of the building. The consuming of energy dose not only lead to deplete energy source in our planet, but also lead to release more amount of CO<sub>2</sub>. So, that increases the globe warming potential and leads planet to creasy weather, beside increasing in temperature. Many sources are available and can be employed as renewable clean energy. And, solar of the sun is one of the important sources. So, many researches and studies have been employed to use the sun energy for cooling and ventilation, not for human

comfort only, but in the industrial and agriculture. Maerefat [1] studied the SC and earth to air heat exchanger (EAHE) to decrease the indoor temperature. Results showed that the performance of the system depends on the solar radiation, outdoor air temperature , beside the configuration between SC and EAHE. With a taller SC in use, the number of required SCs decreases. Other side employed taller SCs lead to uncomfot. Same study was hinted for the optimum EAHE design for 0.5 meter in diameter and 20 meter in length. Maerefat [2] numerically studied for a combined system employing a SC with evaporative cooling cavity (ECC). Results revealed that the integrated system led to good conditions at daytime in test room, even

at high ambient air temperature about 40 °C, with low solar intensity of 200 W/m<sup>2</sup>, and relative humidity of 50%. Ventilation rate influenced by ambient temperature and solar intensity and configuration between both SC and ECC. Wasfy [3] work, a simulation performance of ventilation and evaporative cooling was studied in hot dry climate, for simulating test room in Baghdad city. Room was supplied by SC from one side, and wet pad from other. Results showed the ability to decrease the temperature inside the room to 10 degrees C, in hot dry climate, where the face of SC oriented to the west. Poshtiri [4] made comparison between two systems (SC-EAHE and SC-ECC). Numerical experiments showed that the SC-ECC system can prepare good indoor conditions, at low relative humidity of ambient air, and cooling demand of the room. Also, it depicted that the system can provide a good thermal condition after sun set. Other type SC-EAHE system results refer to that, at high ambient temperature and cooling load, system can provide a good indoor condition even at high air temperature and low solar intensity. Presented a comparison between two systems limited the ability to use the SC-EAHE for low insulation building, while the best choice for SC-ECC system is with high insulated building, especially in dry climates. Hassan [5] Showed results of a case study in Assiut City, for SC and evaporative cooling. Results showed the effect of air flow rate, by the relation between solar radiation, pressure coefficient with area of solar collector. Air flow rate increased when collector's temperature increased, the test room temperature decreased by 10-11.5 °C from the outdoor temperature, in the test day 21may-21 August. Mizanur [6] Presented an experimental work, applied a new design of passive solar chimney with a modern configuration of EC. Where the air induced through the SC leads the outside hot air to pass through the pipe that immersed in outdoor splash water pool. For manipulated air, the temperature decreased approximately 5 °C below the ambient temperature, and about 2-3 °C below the room temperature. Fazel [7] produced a new configuration of passive cooling system through ventilation mode. The system reduces test room temperature of up to 5 °C from the atmospheric temperature, with ability to decrease room temperature during night ventilation.

## 2. Experimental Set Up

### 2.1. Rig Set-Up

The rig that used in this work consists of insulated test room, two types of solar chimneys

(SC) that joint together in series configuration; a vertical fixed SC, and tilted one with 45° in angle, both instilled at the south oriented wall. As well as evacuated tubular collectors with thermosyphos array are used. Good accuracy measurement instruments tools are used in different measuring, beside two types of data acquisition data logger DAQ.

#### 2.1.1. Semi Full Scale Test Room and the Effective Dimensions of the System

The test room with dimensions (2m length, 1.5 m width, 1.5 height), supported by SC's in the south oriented wall, while paper fill (pad) inserted inside vent window and covered by wind protection in north oriented wall. The length of room is bigger than from width and height, to clarifying the behavior of temperature distribution inside room. The structure of test room consists of a wooden frame, walls are insulated by 4 cm of cork with 0.043 W/m. k in thermal conductivity, 2.5 cm thick with 0.05 W/m. k for glass wool. The outside walls are insulated by marmox with  $U=2.7$  W/m<sup>2</sup>.C, while the roof and floor are insulated by marmox thermo-block with  $U=1.69$  W/m<sup>2</sup>.°C. Fig.1, shows EC paper fill (pad), Fig.2. depicts room general details in ISO view, and Fig.3, shows the ETC with characteristics given in table.1. Fig.4. describes the schematic diagram for the test room in vent and EC-mode, that provided with two types of solar collectors instrumented with number of velocity and temperature sensors, table.1, defines all the symbols of Fig.2.

#### 2.1.2. Evacuated Tubular Collectors (ETCTS)

Ten pieces of ETC with Thermosyphon (ETCTS) are used to collect heat at an inclination angle of 45°, and transfer heat to the bottom of the vertical SC. ETC 50 cm in length and 5.8 cm in diameter is shown in Fig.3. TS consists of the condenser which instilled inside the TESB, TS's evaporator is inserted in the axial center of double glass ETC and covered by thin aluminum fin. expander tube with expander roll tools are used to make a good contact between TS's condenser and (CFM) in TESB.

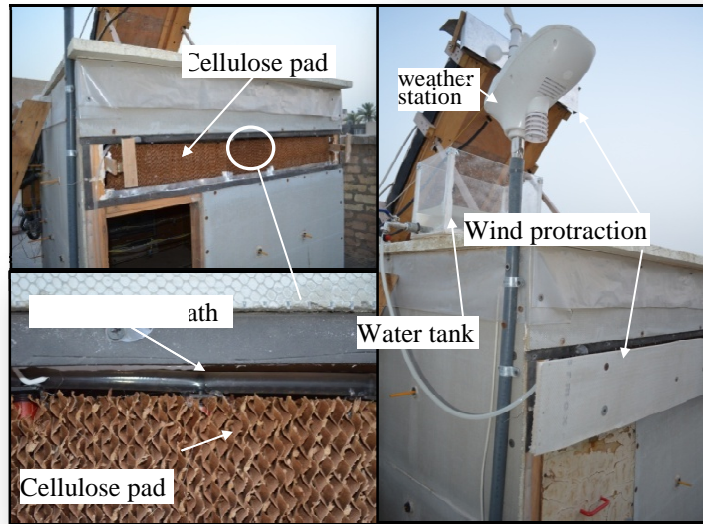


Fig.1. Vent open window covered by paper fill in Evaporative Cooling mode

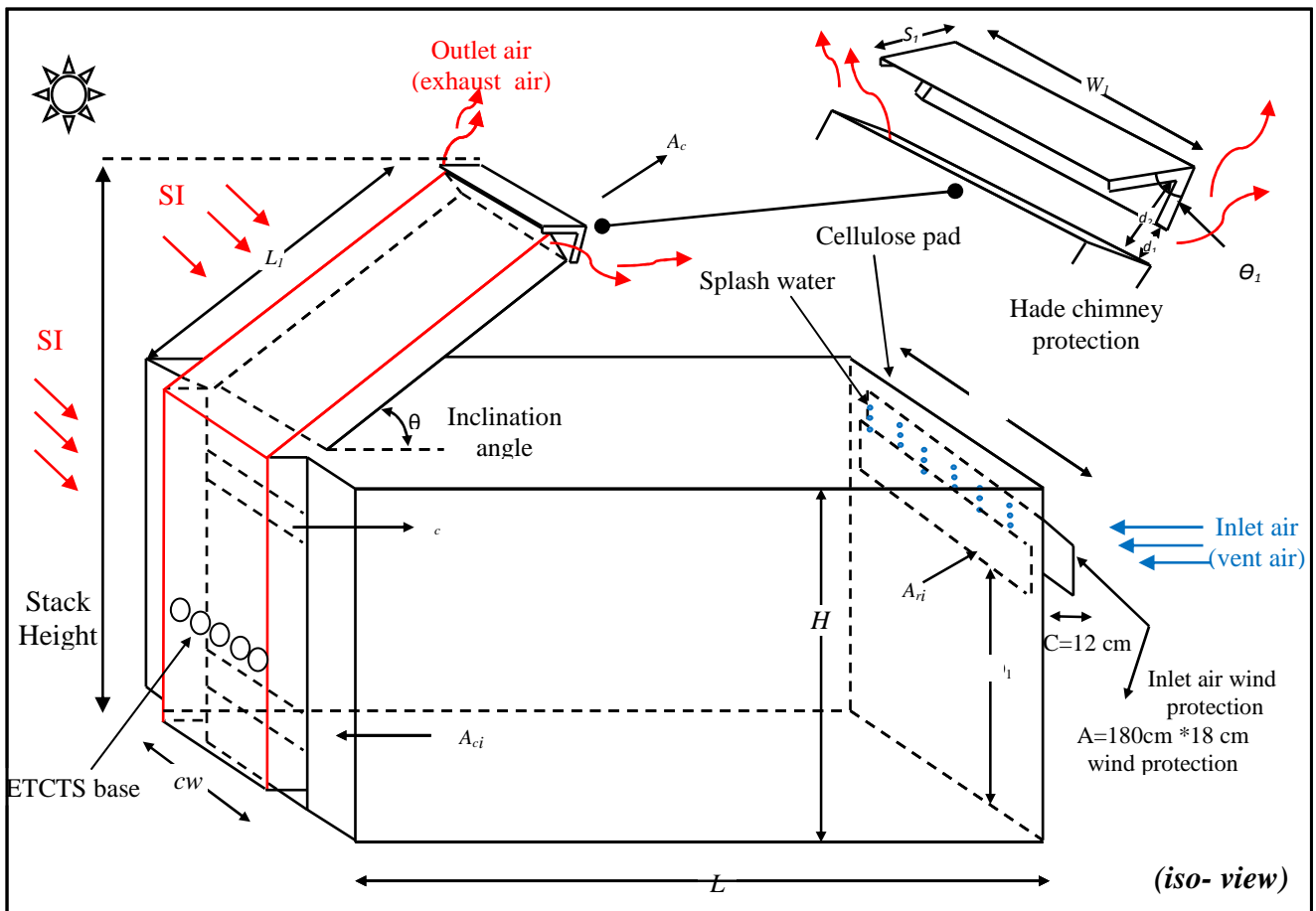
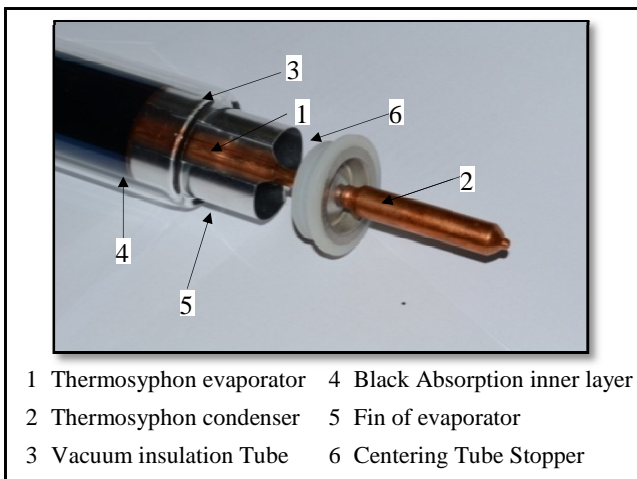


Fig. 2. Schematic diagram of insulated test room.

**Table1,**  
Description of symbols shown in Fig. 2 .

No	Symbol	Description	Dimension	No	Symbol	description	imension
1	w	Width of the test room	148 (cm)	12	CG	Chimney gap	6.7 (cm)
2	H	High of the test room	147 (cm)	13	THS-B	Thermal heat storage box	(thick=2.7cm* w=75cm*H=102cm)
3	L	Length of test room	200 (cm)	14	$A_{ci}$	Area inlet to the chimney	(75m*11cm)
4	CW	Chimney width (THSBW)	75 (cm)	15	$A_{co}$	Area outlet from chimney	(75cm*8cm)
5	$L_1$	Second system chimney height	150 (cm)	16	$A_{ri}$	Area inlet test room	(148cm*16)
6	$W_1$	Head Chimney protection width	91 (cm)	17	$T_{THSB-i}$	Inside temperature	(°C)
7	$\theta_1$	Head chimney protection angle	90 (°)	18	$T_{THSB-S}$	Surface temperature	(°C)
8	$S_1$	Head chimney protection side length	20 cm	19	$T_{THSB-SC}$	Covered surface temperature	(°C)
9	$d_1$	Head chimney distance between lower side corner and exit of moved chimney	4.5 (cm)	20	$T_{air-in-c}$	Temperature air inlet chimney gap	(°C)
10	$d_2$	Head chimney distance between top corner and exit of moved chimney	18 (cm)	21	$T_{air-out-c}$	Temperature air outlet chimney gap	(°C)
11	$LO_1$	Height from $A_{ri}$ to the base	115 (cm)	22	C	Wind protection space from window	12 cm



1 Thermosyphon evaporator    4 Black Absorption inner layer  
 2 Thermosyphon condenser    5 Fin of evaporator  
 3 Vacuum insulation Tube    6 Centering Tube Stopper

**Fig. 3. Evacuated Tubular collector with description notes.**

0.75 meter in width. The box filled by copper foam matrix (CFM), and full refined paraffin wax, to form a thermal energy storage. Upper half of box is covered by double acrylic clear glass from outside, lower halve part is thermally insulated, and connected to ten evacuated tubular collectors, of 50 cm length tilted at 45°. The upper side of TESB that exposed to the sun light is painted by a thermally matt black paint. The other side of the storage box (room side) is covered by a acrylic sheet, with 6.7 cm gap space and 14.92 in aspect ratio. Fig.5. shows steps for manufacture the vertical fixed solar chimney.

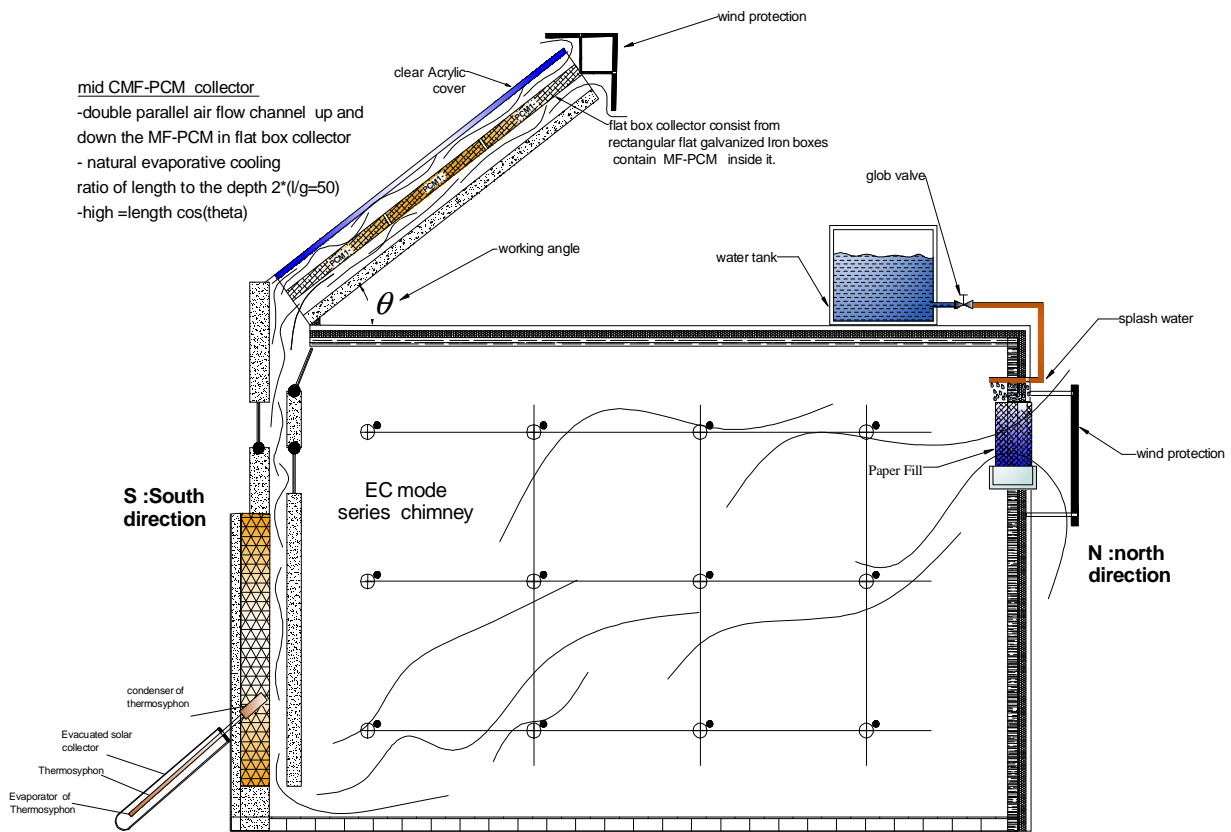


Fig. 4. Schematic diagram describing the test room in vent and evaporative cooling mode.

### 2.1.3.The Solar Chimney (SC)

Two systems of solar chimneys are used, in ventilation with evaporative cooling mode:

#### A-A vertical fixed solar chimney system

Vertical built-in chimney for ventilation and EC mode. A one meter in height of galvanized iron box collector installed at the south oriented wall with 0.75 meter in width. The box filled by copper foam matrix (CFM), and full refined paraffin wax, to form a thermal energy storage. Upper half of box is covered by double acrylic clear glass from outside, lower halve part is thermally insulated, and connected to ten evacuated tubular collectors, of 50 cm length tilted at 45°. The upper side of TESB that exposed to the sun light is painted by a thermally matt black paint. The other side of the storage box

(room side) is covered by a acrylic sheet, with 6.7 cm gap space and 14.92 in aspect ratio. Fig.5. shows steps for manufacture the vertical fixed solar chimney.

#### B-A tilt solar chimney system

Inclined SC at 45° is used by combining with the fixed vertical chimney system. tilted SC consists of a three TESB made from iron galvanized boxes that painted by a layer of matt black and filled with CFM and semi refined of paraffin wax as PCM. The three boxes are arranged in series configuration along the length of SC and construct a double side chimney gap, with 3 cm in each gap wedth.



Fig . 5 Stages to manufacture the vertical fixed SC and setup in the test room.

Outline dimensions for tilted SC are 1.5 m in length and 0.75 m in width as shown in Fig .6,The schematic diagram is shown in Fig .7.

SC's boxes covered by 0.4 cm of acrylic clear sheet.

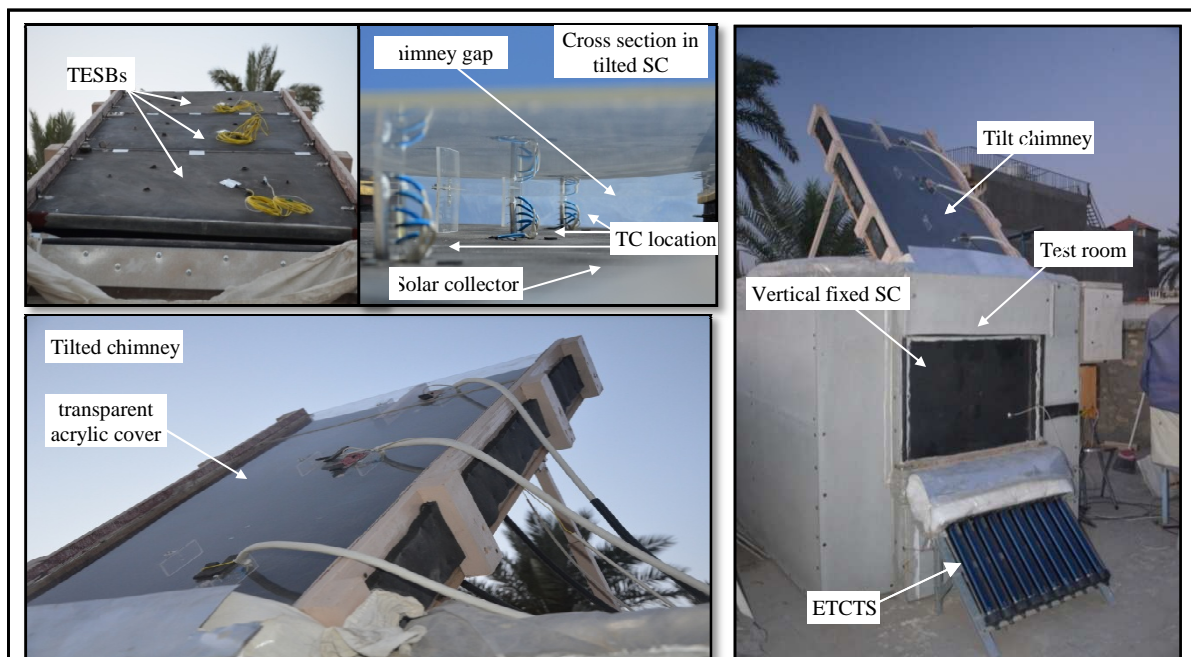
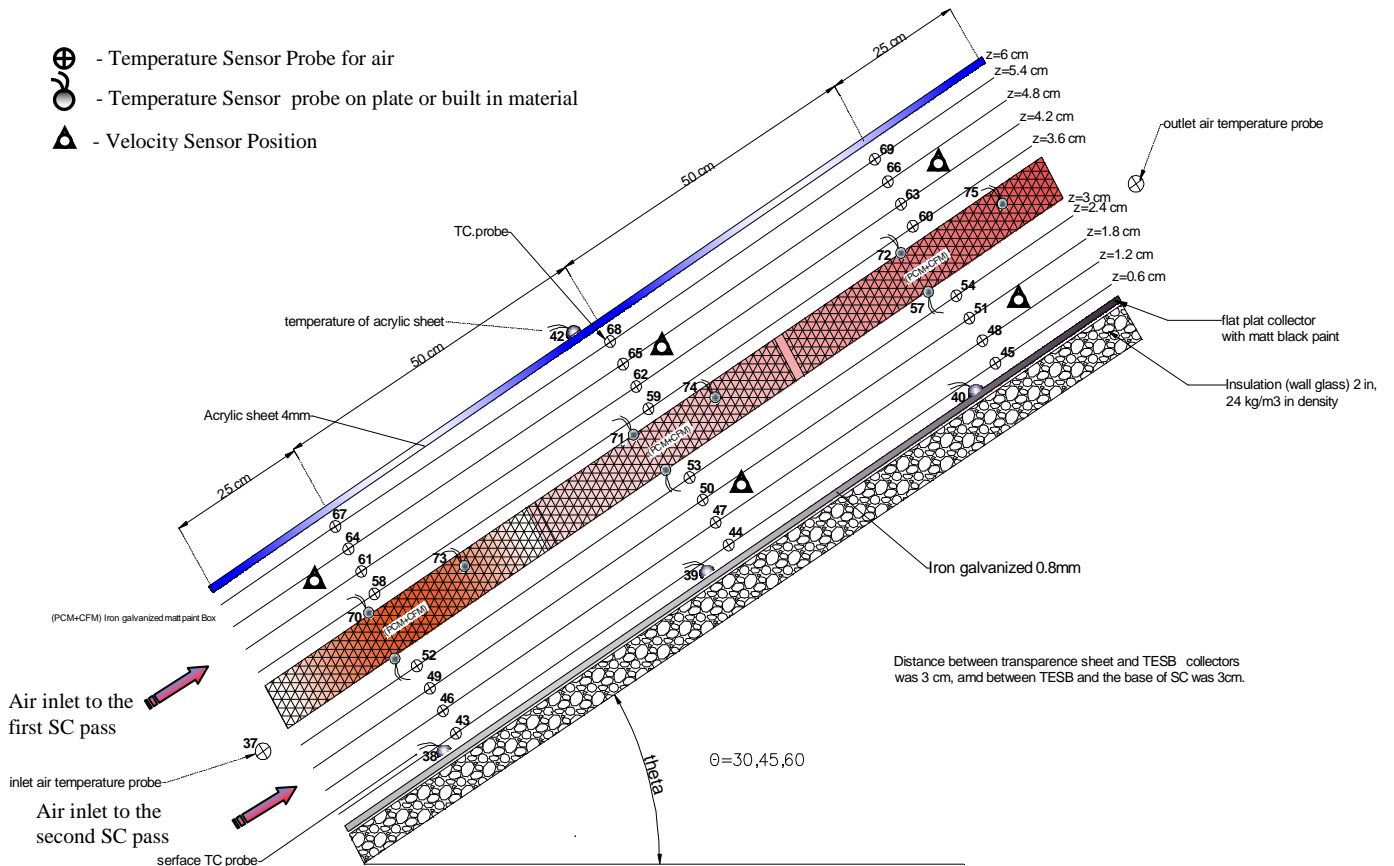


Fig . 6 Setup the inclined SC in the test room

Induced air flows through a double pass over flat thin TES box mid collector, with 50 in aspect ratio for each pass, and that bigger than the

critical aspect ratio ( $ar_{cr}=12$ ), to prevent back flow.



## 2.2. Solar Chimney Components

### 2.2.1. The solar chimney type and working angle in selective mode

In this study, an experimental and theoretical examination are applied, to select the active working angle for tilted SC. Right angle means a good contact between air flow and SC collector without separation, but this angle conjugating simultaneously with low solar intensity. Experimental result, beside theoretical Fig.10 program simulation result refer to choice angle, at 45° as selective working angle in this study. Also in this work, experimentally examining covers three types of inclined 45° SCs; (flat plate, flat plate with double pass, flat thermal energy storage box with double pass). All testes applied for vent mode only. Results in Fig.11 refer to the ability of flat plat collector with double pass, to release heat to air, but with no effect in

night time, so flat box collector with double pass is the active SC collector to employing in vent and EC mode.

### 2.2.2. The absorber

One TESB are used as SC collector in vertical chimney, while Three TESBs are used to construct the tilted chimney collector. The emissivity of the painted layer of plate is  $\epsilon=0.095$ . and the absorptivity  $\alpha_p=0.9$ , while the reflectivity  $\rho_{plate}=0.1$ .

### 2.2.3. Thermal energy storage material

A combined of paraffin wax, as a phase change material, and copper foam matrix are used as a TESM. Where the paraffin wax is used to storage heat, in sensible and latent heat regions, while the CFM is used to enhance the thermal conductivity of thermal TESM.

**2.2.4. Phase change material (PCM)**

Many types of paraffin and microcrystalline wax are examined to find the suitable wax. So two types of paraffin wax are selected as working PCM;

-First type a full refined paraffin wax PW-600, used as a TESM with a CFM. This type is used in the fixed vertical SC.

-Second wax type is a semi refined paraffin wax, used with the CFM as a TESM in the TESB for the second inclined chimney. To define the

thermo physical properties of each wax, by limiting the melting point for each experimentally from (temp-time) diagram Fig.8.

Then by using empirical relations that dependent on the number of carbons. Where from the melting temperature and from table-2 [8], can be select the suitable wax, then calculated the properties for solid, liquid single zone and mushy zone. The formula defined n-Alkanes structure is  $C_n H_{2n+2}$ , n means the number of carbons.

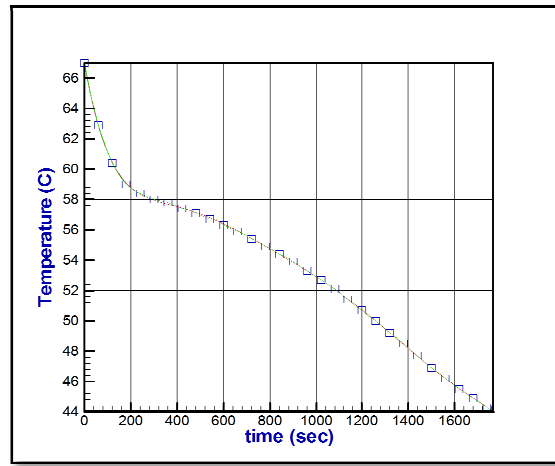
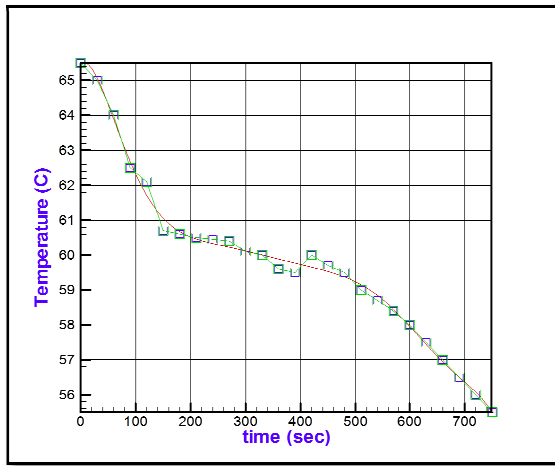


**Fig. 8. Experimental results show behavior of wax in different temperature  
a, full refined PW b, semi-refined PW**

	Specific Heat Liquid (J/mol.K) at 353 K	Boiling Point (K)
	698 <sup>a</sup>	629.7
	739.0	641.8
	772.0	653.4
	805.0	664.5
	815.9	675.1
	870.0	685.4
	928 <sup>a</sup>	695.3
	937.0	704.8
	1001 <sup>a</sup>	714.0



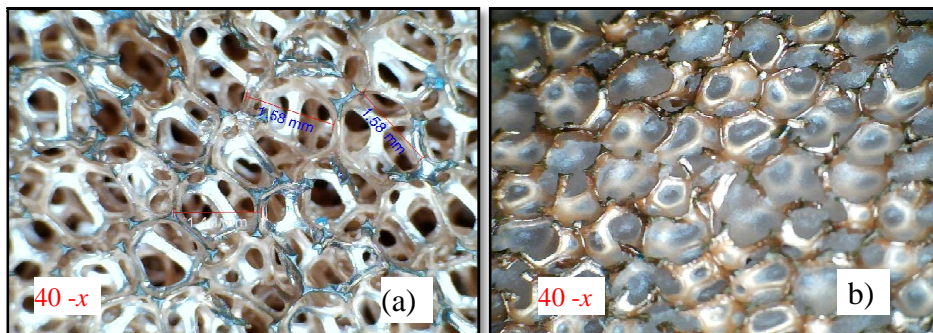


Fig. 9. Copper foam matrix a-with PW, b-without PW.

### 2.2.5. Copper Foam Matrix (CFM)

The combined of FM-PCM means higher thermal conductivity, with same latent heat of fusion, and same solidification and melting temperature. So, a copper foam matrix CFM is

used to enhance the heat transfer, because the thermal conductivity of PCM is not enough to receive or release heat in selective heat transfer duration time. Fig .9, refers to the CFM with and without PCM. CFM used with 95% porosity and 30 porous per inch (30 ppi).

Table 3, physical properties for Acrylic and commercial window glass( Bk7).

	Angle (degree)	n	$\tau$	$\rho$	$\alpha$	KL	$\epsilon$	K (w/m.°C)
Glass BK7	30		0.799	0.072	0.125			
	45	1.526	0.782	0.0875	0.133	32*L at 4mm	0.92	0.81
	60		0.729	0.14	0.141			
Clear Acrylic	30		0.885	0.0741	0.0414			
	45	1.491	0.872	0.0868	0.0443	0.04	0.94	0.7
	60		0.82	0.143	0.0477			

L: cover thickness in mater.

n: Average refractive index in solar spectrum of cover materials.

K: extinction coefficient

$$\tau + \rho + \alpha = 1$$

$\tau$ = transmittivity,  $\rho$ =reflectivity

$\alpha$ = absorbtivity,  $\epsilon$ = emissivity

### 2.2.6. The transparent cover

Nontraditional transparent cover, 4 and 6 mm from clear acrylic sheets are used with vertical and tilted 45° SCs. The special properties for these material are the; flexibility, light weight, anti crash, beside other properties that in common with BK-7. All important properties for acrylic and BK-7 except thermal conductivity of BK-7, are calculated for three selective angles and listing in Table.3, that showing a comparison between commercial glass sheet (BK-7) and clear acrylic sheet.

### 2.3. Measurement and instrument tools

The following measurement and instrument devices are used in this project beside data logger, data acquisition (DAQ), to measuring the depended and independent variables;

#### 2.3.1. Temperature

Three types of temperature sensors are used in different positions. With 290 meter of type-K thermocouple (TC) are used to cover all the temperature that must be measured in the SC's and test room beside the SC's gap. A 3D mesh grid of temperature sensors are distributed inside

the test room. 36 semiconductors type LM-35dz, with 36 thermocouple probes are distributed inside the room in three horizontal layers (3\*4) node. The probes are connected to two types of Data Acquisition (DAQ) from labJack U6-PRO and UT-7, also two types of digital thermometer are used

- DM6801A+ digital thermometer with 0.1 °C in resolution and -50 to 199 °C in range, with +/- (0.2%+1 °C) value in accuracy.

- DM6803A+ digital thermometer with 0.1 °C in resolution, 0 to 800 °C in range, and accuracy with +/- (0.3%+1 °C). Both thermometers are connecting to the selector switch. As well as, array of thermocouple probes are distributed and connected to the vertical and tilted SC's gab. TC's probes connected to the collector plate, TESB, ETC and glass cover. Fig .7 shows The positions array of thermocouple probe sensors in tilted SC.

### 2.3.2. Air Velocity

Two types of a thermal digital anemometer with high resolution are used to measure the air velocity in the two systems of chimney gap, beside room.

-TSI AVM410 thermal anemometer with 0.01 m/s in resolution, and same value in threshold. Velocity range (0 to 20 m/s), and reading temperature range (-18 to 93 °C).

-Testo 405-V1 Thermal anemometer with 0.01 m/s in resolution and threshold, while velocity range (0 to 5 m/s) at (-20 to 0 °C) and (0 to 10) when temperature range (0 to 50 °C).

- AM-4838 digital fan anemometer is used primary to limit the direction of air flow inlet to or outlet from the solar chimney beside smoke generator. The specification of this digital anemometer : 0.1 m/s in resolution, 0.4-30 m/s in range and threshold equals 0.4 m/s. Positions of the measured velocity are showed in Fig.7, where a three-hole port to measure the velocity from upper side air pass, and two from lower side are pass .

### 2.3.3. Solar radiation intensity

Two types of solar intensity meter are used in the experimental work. TES- 1333 model is fixed at tilted SC, with specification: 1 W/m<sup>2</sup> in resolution, 0-2000 W/m<sup>2</sup> in range. Other Type TES-132 with a data logger and interface connection to PC. Its specification: 0.1W/m<sup>2</sup> in resolution and measuring range 0-2000 W/m<sup>2</sup>. This type Is used to measure the solar intensity before and after the acrylic cover to calculate the

transmittivity value. Beside recording solar intensity on surface of ETC and fixed SC. Average solar intensity recorded by WS.

### 2.3.4. Weather station system

A modern weather station model *WS-1000-WiFi* with 915 MHz in Frequency, outdoor and indoor instrument collection, transmitted the data every 16 second to the analyzer data logger data screen, with built in memory, and external data storage. Data logger records the data transmitted at interval time, that recognized by user to record data each 60 seconds for 24 hour. The following important data can be recorded by the *WS-1000-WiFi* :

- Indoor average temperature
- Indoor relative humidity
- Real and absolute pressure
- Outdoor average temperature
- Outdoor relative humidity
- Solar radiation intensity (horizontally)
- Wind speed
- Gust speed
- Wind direction

### 2.4. Experimental Test Procedure

The experimental work, is achieved in June, 2015, where data are logging for the dependent variables along 12 hours. All measurement and instruments tools are used as mentioned previously to measure and record the dependent variable, for each 2 hours as test interval, and average value for general variables that measured and recorded by WS data logger along 24 hours, with 20 minutes as test interval

The depended variables including each of

- Measuring temperature in; chimneys gap, test room space, TESB, outdoor temperature,
- velocity in chimney gap beside inlet and outlet SC
- solar intensity.

While the general depended variable including each variables that measuring by WS.

Many conditions are Applied, to select test day such as; clarity (not dusty), acceptable wind speed without gust, the clouds absence or partial cloudy day.

## 2.5. Theoretical Consideration and Calculation

In this study assuming there is no heat losses directly from test room to the surround, or from the insulated parts of SC's. Therefore, SC that exposure to the sun solar, absorbed all heat with respect to the value of collector absorbtivity, reflectivity and emissivity, beside the acrylic cover's transmittivity, absorbtivity, reflectivity and refractivity value. So, according to the heat balance, heat absorbed by collector must be equal to heat released to the working air that passes through the chimney gap.

### 2.5.1. Calculated heat storage (TESB)

In experimental test, results are shown in Fig.8, to find melting point range, then from n-Alkenes table-2 [8], to define the latent heat of fusion vale in mushy zone. So for material which has a symmetrical distribution of the specific heat for the melting region[9],

$$\therefore T_m = \frac{T_s + T_l}{2} \quad \dots(1)$$

$$h_{sl} = h_l - h_s \quad \dots(2)$$

where  $h_{sl}$  defined from wax diagram and n – Alkanes table

$\rho_l, \rho_s$ : paraffi wax density for liquid and solid

$$h(T) = c_{p,s}T + \eta_s \quad T < T_m \quad (\text{solid})$$

...(3)

$$\eta_n = \left(\frac{h_l - h_s}{2}\right) e^{\left(-2\frac{|T - T_m|}{\tau}\right)} \quad n \in [s, l] \quad \dots(4)$$

$$c_p = \frac{1}{\rho_D} (0.388 + 0.00045 * (1.8 * t + 32)) * 4186.9 \quad \dots(5)$$

$\beta$ : inclination [-]

$\rho$ : density [ $\frac{kg}{m^3}$ ]

$\tau$ : width of melting zone [K]

$T_{pw}$ : PW temperature [K]

PW: paraffin wax

$h$ : enthalpy [ $\frac{kJ}{kg}$ ]

$s$ : solid

$l$ : liquid

$m$ : melting

as defined before,  $\frac{\tau}{2} = \tau_s = \tau_l$  for materials which show a symmetrical distribution of the specific heat for the melting region.

$$\therefore \tau = T_l - T_s \quad \dots(6)$$

For mushy region to calculate the specific enthalpy,

$$h(T) = c_{p,constant} \cdot T + \frac{h_l - h_s}{2} \times \left\{ 1 + \tanh \left[ \frac{2\beta}{\tau} (T - T_m) \right] \right\} \quad T_s \leq T \leq T_l \quad (\text{mushy}) \quad \dots(7)$$

So, the specific heat capacity is the dervative of specific enthalpy then

$$c_p(T) = c_{p,constant} + \frac{h_l - h_s}{2} \times \frac{\frac{2\beta}{\tau}}{\cosh^2 \left[ \frac{2\beta}{\tau} (T - T_m) \right]} \quad \dots(8)$$

For liquid region to calculate the specific enthalpy

$$h(T) = c_{p,s}T_m + (h_l - h_s) + c_{p,l}(T - T_m) - \eta_l \quad T > T_m \quad (\text{liquid}) \quad \dots(9)$$

to calculate heat transfer in evaporative cooling procedure [10]. Cooling and humidification (removed heat (sensible) with the addition of moisture (latent)) are:

$$Q_{total} = Q_s + Q_l \quad \dots(10)$$

$$Q_{total} = \dot{m}_{air} \{ c_p(T_F - T_O) + h_{fg}(W_F - W_O) \} \quad \dots(11)$$

### 2.5.2. Heat transfer to the humid Air

The inside solar chimney heat transfer from TESB to the moist air by simple equation is illustrated below [10].

$$Q = \dot{m}^o c_p (\Delta T) \quad \dots(12)$$

For the sensible heat transfer to the dry air,

$$Q_{total} = \dot{m}^o (C_{p-g} \cdot t + w h_w + w C_{p-w} \cdot (t - t_{ref})) \quad \dots(13)$$

Or by employing the equation of state for moist air [10].

### 2.5.4. Simultaneous efficiency

To compute the simultaneous efficiency at duration time of heat charge, it must compute the rate of heat storage in TESB during its exposure to the solar radiation which can be calculated from eqn. below [8]

$$q = m \frac{\Delta h}{t} =$$

$$m_{wax} \Delta h_{wax} + m_{copper} C_{copper} \Delta T_{copper} \quad \dots(14)$$

$m$ = mass for wax and copper foam matrix

$t$ = duration time to charge TESB by heat ( $q$ )

so, the heat storage in duration time  $t$  can be found from eqn. (15)

$$Q = q \cdot t \quad \dots(15)$$

To compute heat storage during duration charge for  $N$  time , by algebraic summation of eqn. 14 to get

$$Q_{total} = \sum_{n=1}^N \{ m_{wax} \Delta h_{wax} + m_{copper} C_{copper} \Delta T_{copper} \} \quad \dots(16)$$

Its mean the rate between heat storage to the heat absorbed by TESB.

$$\eta = \frac{Q_{storage}}{Q_{absorbed}} = \frac{\{m_{wax}\Delta h_{wax} + m_{copper} C_{copper} \Delta T_{copper}\}}{I_{beam} \cdot A_a \cdot \alpha_a \cdot t} \quad ..(17)$$

### 2.5.5. Ventilation air change per hour (ACH)

To calculate the mass flow rate through the solar chimney only, or through the solar chimney and room. [11],[12].

$$m^o = V_{f,o} \rho_{f,o} A_o = C_d \frac{\rho_{f,o} A_o}{\sqrt{1+(A_o/A_i)}} \times \sqrt{2g L_c \left[ \frac{T_f}{T_r} - 1 \right]} \quad ..(18)$$

Where,  $C_d$  is the system's discharge coefficient, is defined as the ratio of the cross-section area at the vena-contract to the actual opening area. It is taken as 0.57 due to the sharp edge inlet, or calculated as shown later.  $T_f$  is the mean temperature of air in the channel (Kelvin), which is described by the equation below [13].

$$T_f = \gamma T_{f,o} + (1 - \gamma) T_{f,i} \quad ..(19)$$

Where,  $\gamma$  is meant for the mean temperature approximation which depends on the inlet and outlet air temperature.  $\gamma = 0.74$ ,  $T_{f,o}$ ,  $T_{f,i}$  are equal temperature of air inlet and outlet solar chimney;  $T_r$  room temperature;

$A_r = A_o/A_i$  ratio between outlet and inlet opening area of SC [14]

$$T_{m1} = \frac{T_g + T_f}{2} \text{ glass side} \quad ..(20-a)$$

$$T_{m2} = \frac{T_A + T_f}{2} \text{ absorber side} \quad ..(20-b)$$

$$T_m = \frac{T_{m1} + T_{m2}}{2} \quad ..(21)$$

To calculate the system's discharge coefficient  $C_d$  [15]:

$$C_d = 0.4 + 0.0045 * |T_f - T_o| \quad ..(22)$$

$T_f =$

temperature of air within the gap ( °K);

$T_o =$  temperature of outside ( °K)

$T_r =$  room temperature ( °K);

$L_c =$  vertical distance between outlet and inlet(m)  $L_c$  in this study calculated as

$$L_c = h_{ch1} + h_{ch2} * \sin(\theta)$$

$h_{ch1} =$  high of vertical chimney - 1;

$h_{ch2} =$  high of inclined chimney - 2;

$\theta =$  Inclination angle of SC from horizontal

To calculate ACH; air change per hour [14] is ACH

$$= \frac{\dot{m}}{\rho_{f,o}} * 3600 \text{ Room Total volume} \quad ..(23)$$

### 3. Result and Discussion

Experimental results showed, the effect of EC system by using induced air through solar chimney. Fig.12. shows that there is a decreasing in indoor temperature along test time comparing with outdoor temperature. Maximum difference in temperature 8.5-9.2 °C occurred at maximum solar radiation with increasing in relative humidity. Fig.13. shows the vent-mode only where indoor temperature is almost higher than outdoor temperature with low RH%, especially in noon time at high solar radiation. Fig.14. appears the effect of induced air through solar chimney, and the evaporative cooling effectiveness (ECE) value, where the high value of effectiveness occurs approximately at high value of solar radiation. That means a high velocity of air through SC (through test room) at noon time.

Temperature distributions in vertical mid layers along test room are shown in Fig.15-(a-i). Fig.15-d. shows 3D test room in three layers : east , mid and west layer along the test room and after 2.pm, the sun direction effect is shown in the west layer, where increasing in temperature more than the temperature of east layer. After sunset starts, Fig.15-f. shows the starting decrease in room temperature. Other Fig.15.(g-i) represents the distribution of temperature in test room along day time and night time, where temperature increasing in the roof and near the solar chimney, while it decreases on other zone especially near the wet pad.

In Fig.16, The experimental and theoretical value of air change per hour (ACH) in EC-mode depends on discharge coefficient of system 0.371, that calculated for the present test room. Low  $C_d$  value caused by the effect of fill pad air flow resistance. In experimental work, ACH was determined, depending on the tilt SC collector temperature and air velocity, so it measured in mid way in chimney gap, and before the end way of chimney gap. The fluctuation appeared in ACH value because of the turbulent in air flow, while the value of theoretical ACH was determined depending on the variables in Eq.23. The variables change smoothly especially temperature of room and collector, while the calculation of mass flow rate of air depends on upper and lower collector temperature and density. So the air mass flow rate was experimentally estimated in upper and lower chimney gap way (mid ,before end), Fig.17.

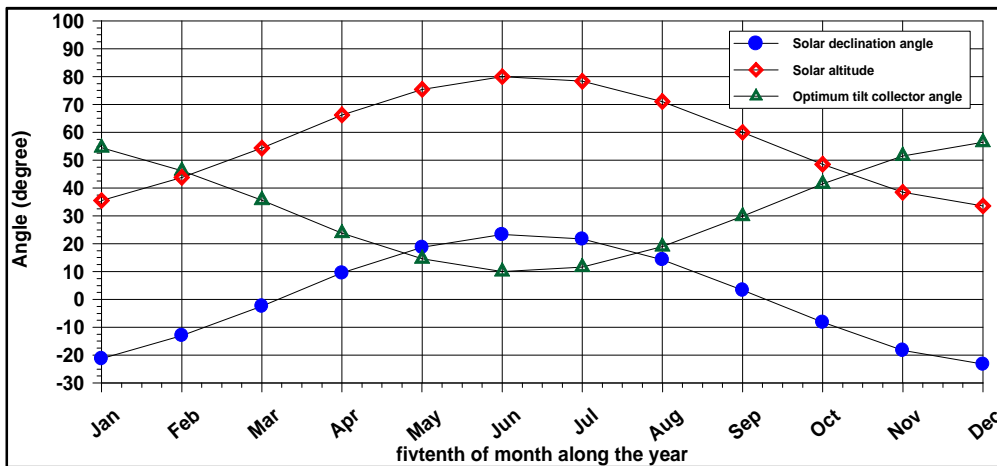


Fig. 10. Optimal solar chimney angle, for different seasons in Baghdad city.

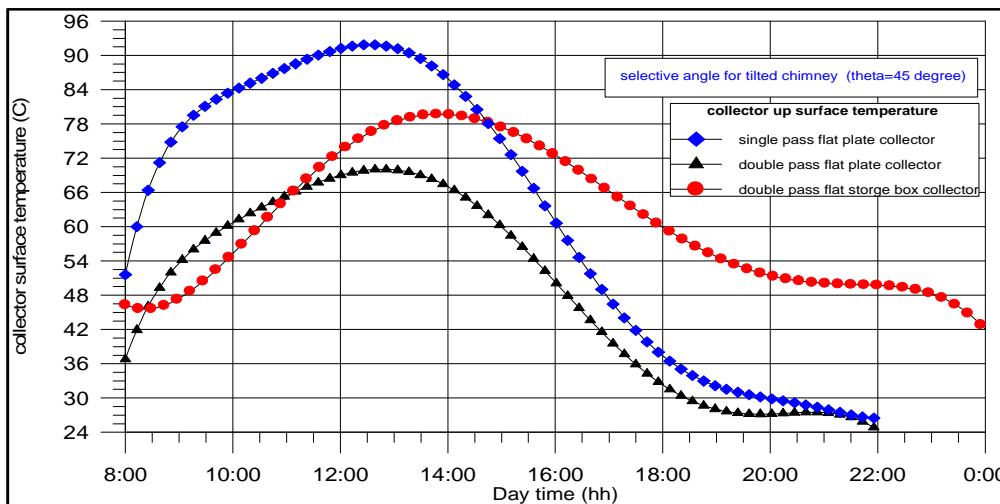


Fig.11. comparison between three different types of tilted solar chimney's collector with selective working angle.

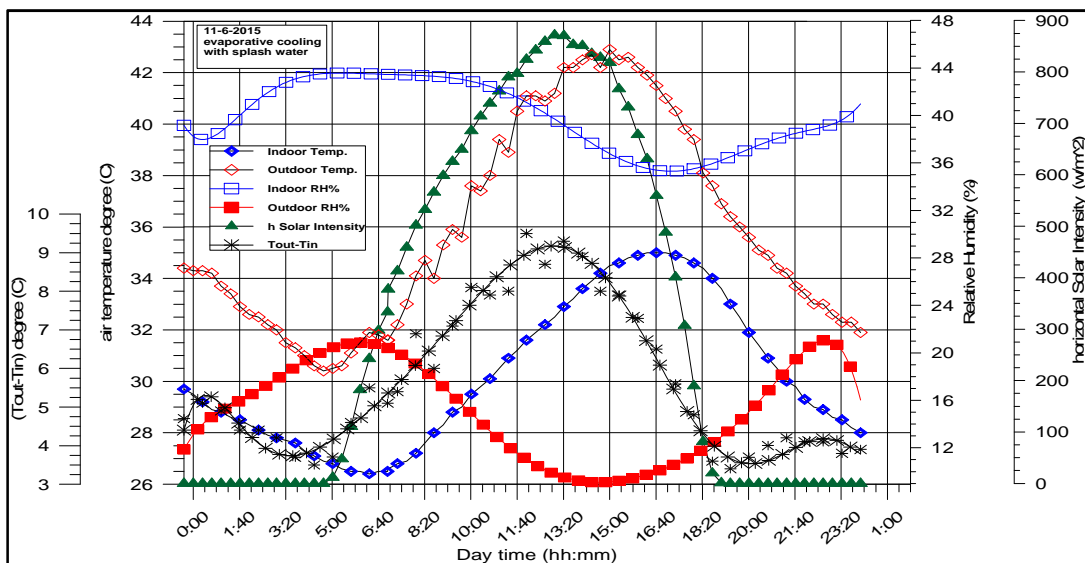


Fig. 12. Average temperature for indoor and outdoor through test day with Vent and EC effect.

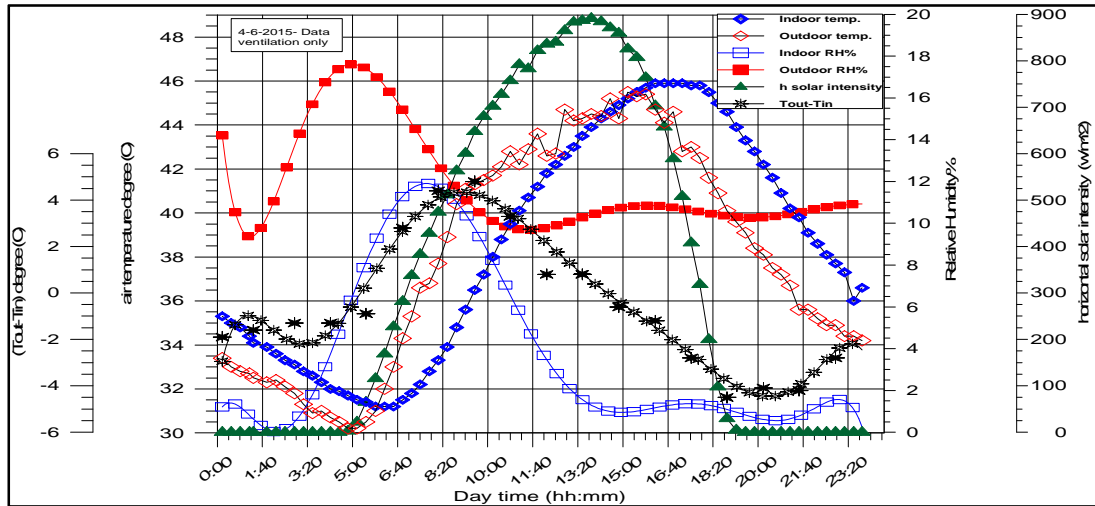


Fig.13 average temperature for indoor and outdoor through test day for Vent only.

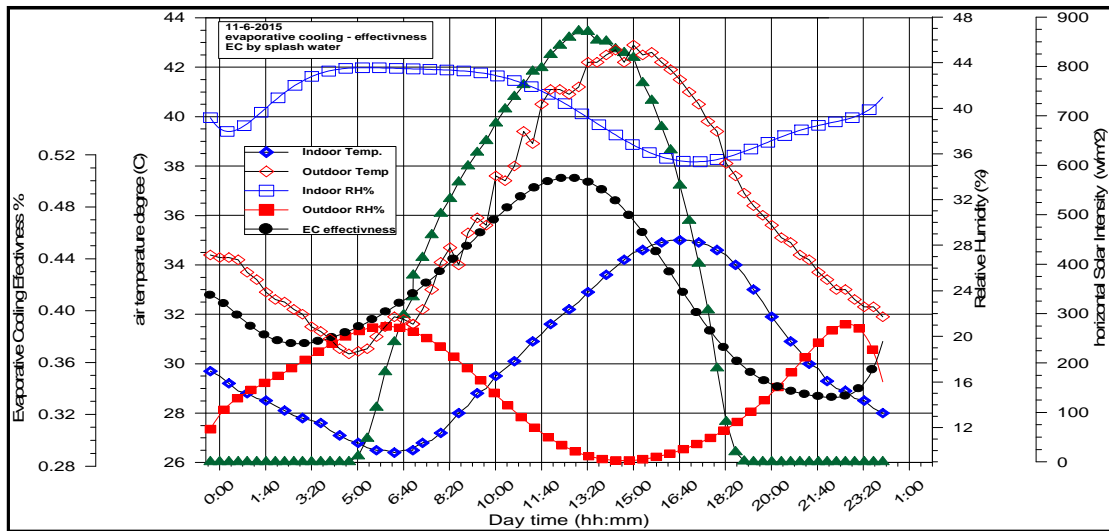


Fig.14. Evaporative Cooling effectiveness through test day.

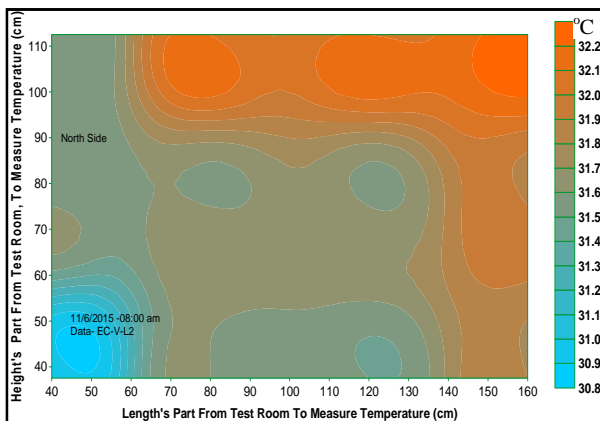


Fig. 15-a. Effect of evaporative cooling on the temperature Distribution in mid layer test room (08:00 am).

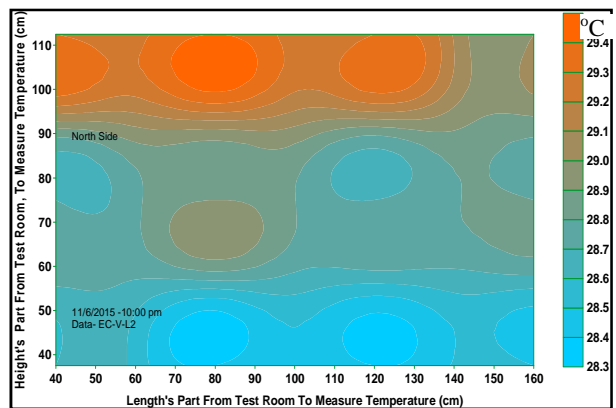


Fig. 15-b. Effect of evaporative cooling on the temperature Distribution in mid layer test room (10:00 am).

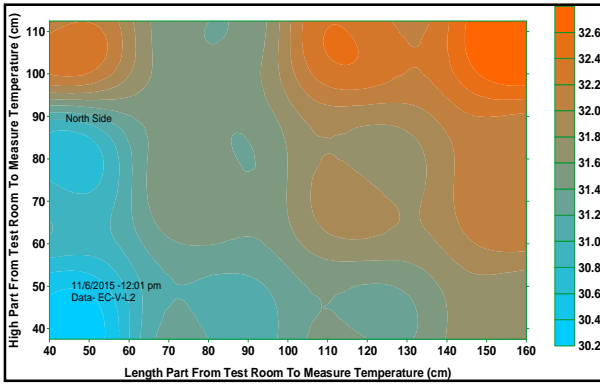


Fig. 15-c. Effect of evaporative cooling on the temperature Distribution in mid layer test room (12:00 pm ).

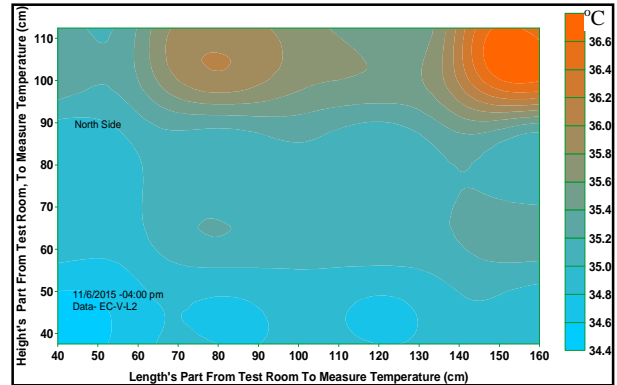


Fig. 15-e. Effect of evaporative cooling on the temperature Distribution in mid layer test room (04:00 pm).

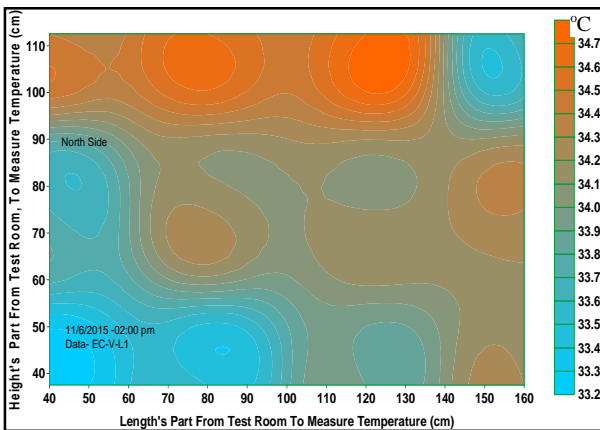


Fig. 15-d. Effect of evaporative cooling on the temperature Distribution in 3D test room (02:00 pm).

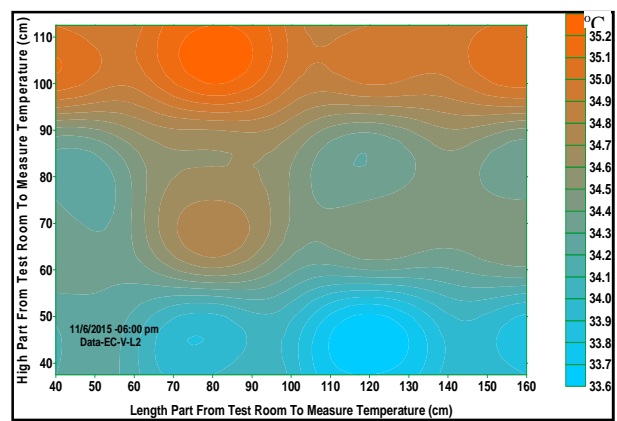


Fig. 15-f. Effect of evaporative cooling on the temperature Distribution in mid layer test room (06:00 pm)

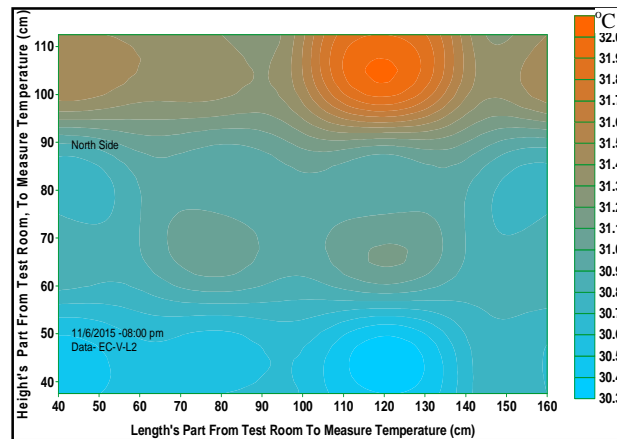
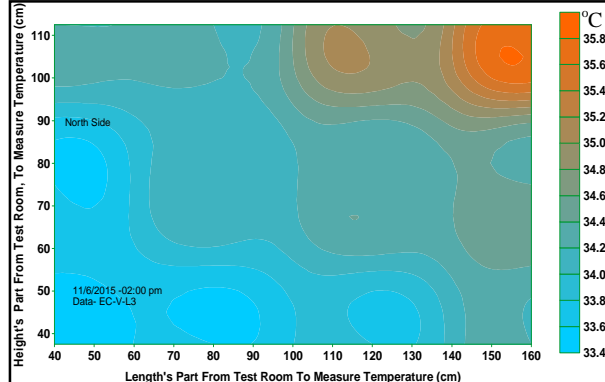
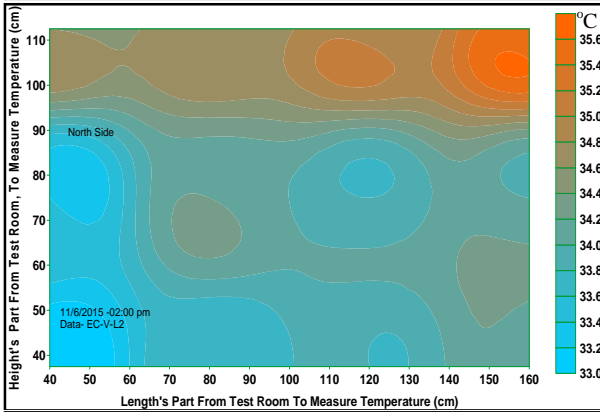


Fig. 15-g. Effect of evaporative cooling on the temperature Distribution in mid layer test room (08:00 pm).

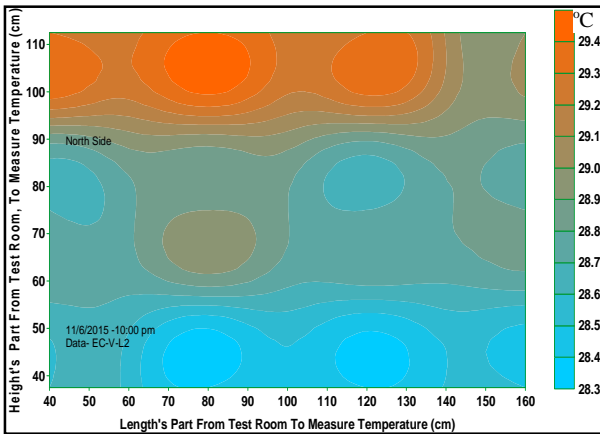


Fig. 15-h. Effect of evaporative cooling on the temperature Distribution in mid layer test room (10:00 pm).

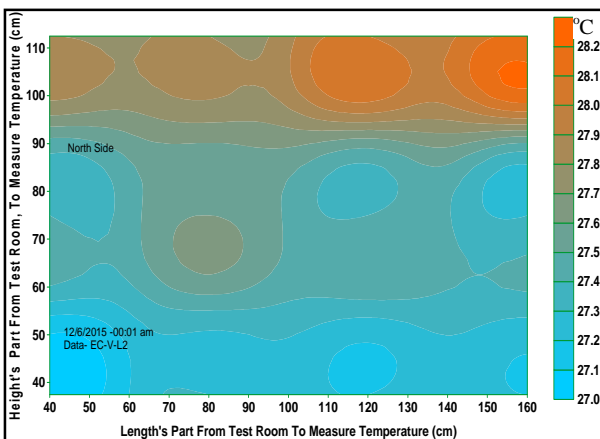


Fig. 15-i. Effect of evaporative cooling on the temperature Distribution in mid layer test room (12:00 am).

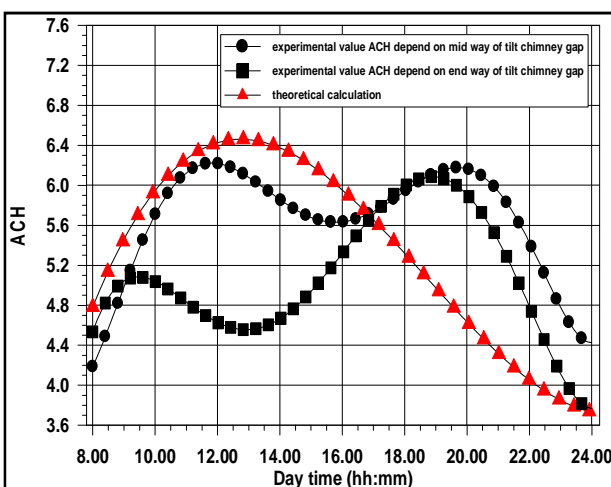


Fig. 16. Air change per hour in evaporative cooling mode.

So, the mass flow rate through the test room is equals to the mass flow rate through the chimney with respect to the synchronous change in value for volume flow rate and density. Maximum of mass flow rate of air through test room approximately  $36.651 \text{ kg}\cdot\text{hr}^{-1}$  in value. Air gap temperature in vertical fixed chimney shown in Fig.18, the air temperature are measured in three positions in chimney gap, after inlet, in the mid way, and before outlet of chimney gap. Results refer to increase in air temperature along the way of chimney length, and the heights of air temperature in same level are near the TESB. Fig.19. shows the heat storage efficiency (HSE) with maximum value in 10:00 am, because the higher difference in temperature between inside TESB, and it's up-surface collector ( $0.75 \times 1.5$ )  $\text{m}^2$  accrues at that time. HSE equals the summation of change of energy storage through time to the summation of solar energy through same time.

#### 4. Conclusions

From the experimental results, the following conclusions can be drawn:

- Employing the evaporative cooling effect, made more successfully comfortable zone ,and more suitable for human live mode, and that done by decreasing the room air temperature with respect to the increasing of relative humidity.

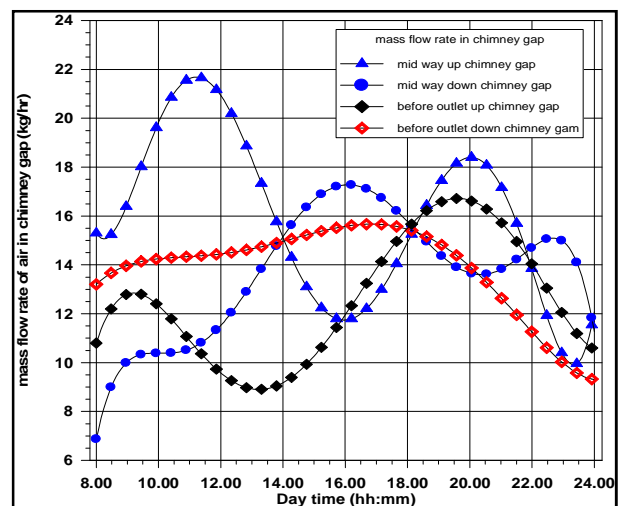


Fig. 17. Experimental value of mass flow rate.

- Comfort condition does not cover the day time only but also the night time by using the thermal energy storage material.
- Accomplished double pass solar chimney collector ensures a good aspect ratio between



chimney length and the gap thickness, the ratio is bigger than 12, make a chance to prevent reverse air flow in chimney gap.

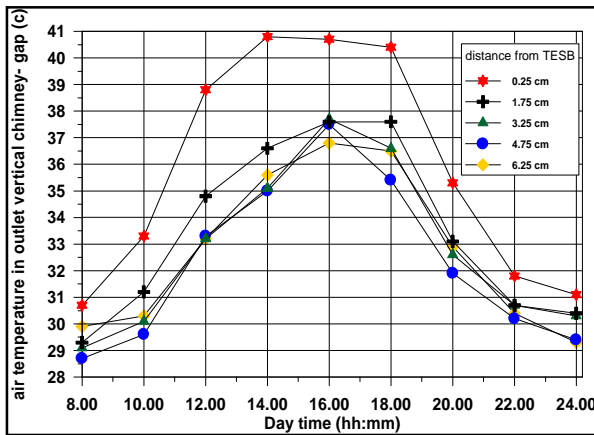
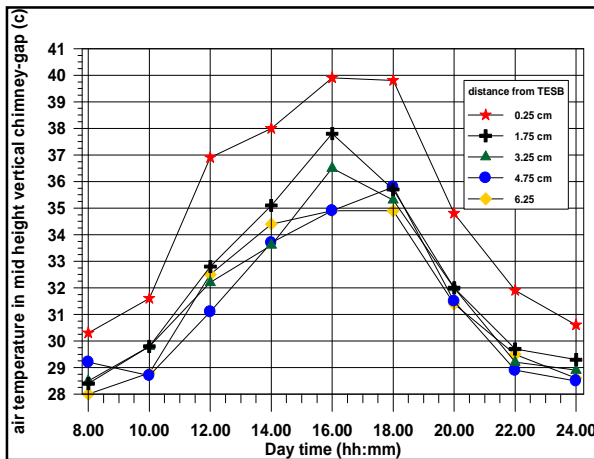
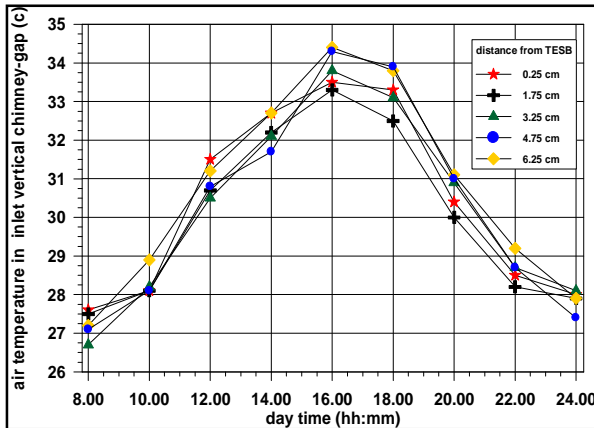


Fig.18. Vertical SC air gap temperature.

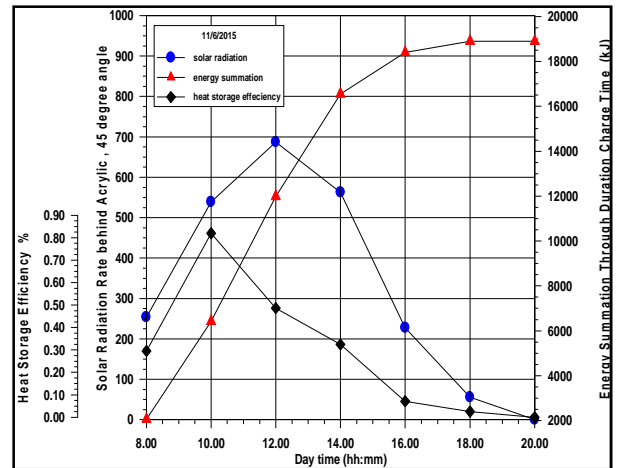


Fig. 19. Solar Radiation, Energy Summation and heat storage efficiency.

Nomenclature

- A area
- ACH Air chinge per hour
- $C_d$  Discharge coefficient
- $C_p$  Specific heat
- EC Evaporative cooling
- ECE Evaporative cooling efficiency
- ETC Evacuated tubular collector
- $g$  gravitational acceleration
- $H$  enthalpy , height
- HSE eat storage efficiency
- $L_{beam}$  beam solar radiation
- $L_c$  characteristic length
- $m$  mass
- $m^o$  mass flow rate
- $P$  Pressure
- PW Paraffin wax
- $Q$  heat
- SC Solar chimney
- $T, t$  Temperature, time
- TESB,M Thermal energy storage-box, material
- $u$  velocity
- $V^o$  Volumetric flow rate
- $w$  Moisture contain

Greek letters

- $\beta$  Inclination
- $\rho$  Density
- $\tau$  Width of melting zone
- $\alpha$  Sun altitude angle
- $\varphi$  Latitude angle
- $\omega$  Hour angle
- $\delta$  Declination angle
- $\theta$  Solar radiation angle,

$\theta$	Solar chimney tilt angle
$\eta$	Heat Storage Efficiency

### Subscripts

a	air
c	Copper
g	gas
$I$	inlet
$l$	liquid
m	melting
o	outlet
s	Solid
$Sl$	Latent heat of fusion

### 5. References

- [1] M. Maerefat, A.P. Haghghi , “ Passive cooling of building by using integrated earth to air heat exchanger and solar chimney”, *Renewable Energy* 35, PP. 2316-2324, 2010.
- [2] M. Maerefat, A.P. Haghghi , “ Natural cooling of stand-alone houses using solar chimney and evaporative cooling cavity”, *Renewable Energy* 35, PP. 2040-2052, 2010.
- [3] Usama Mustafa , “Using Solar Chimney to Suck Air Through a Wet Ped”, *Journal of Engineering and Development*, Vol. 15, No.2, PP. 205-213, June-2011.
- [4] Amin H. Poshtiri, Neda G., “ Comparative survey on using two passive cooling systems, solar chimney- earth to air heat exchanger and solar chimney-evaporative cooling cavity”, *World Renewable Congress*, PP. 2102-2109, 2011, Sweden.
- [5] Amr S., Hiroshi Y., Tomonobu G., “Integration of Evaporative Cooling Technique With Solar Chimney to Improve Indoor Thermal Environment in the New Assiut City, Egypt”, *International Journal of Energy and Environment Engineering*, PP. 1-15, 2013.
- [6] MD. M. Rahman, Muhammad M.,” A passive cooling system of residential and commercial buildings in summer or hot season”, *Recent Advances in Renewable Energy Source*, PP.100-105.
- [7] Md. F. Rabbi, Mrittunjoy Sarker, “Alternative Room Cooling System”, *American Journal of Engineering Research (AJER)*, Vol. 4, Issue-6, PP. 215-218, 2015.
- [8] Arkan U.Meko, ”Energy Storage by phase change by using paraffin wax”, MSc, thesis, *Machines and Equipment*, University of Technology, Baghdad, Iraq, 2004. (Arabic)
- [9] Helmut E. Feustel , Corina Stetiu, ”Thermal Performance of Phase Change Wallboard for Residential Cooling Application”, *Environmental Energy Technologies Division*, Ernest Orlando Lawrence Berkeley National Laboratory, University of California Berkeley, CA 94720, USA, 1997.
- [10] S. Salam, et al., “Psychometric Analysis for arbitrary dry-gas mixtures and pressures using microcomputer”, *ASHRAE Transaction*, Part-1, Vol. 92, 1986.
- [11] Hussain H. Al-Kayiem, Ahmed K. Hussein, Toh Seng Peow, “Investigations of Natural Convective Heat Transfer in Rectangular Thermal Passages”, *International Journal of Mechanical, Aerospace, Industrial and Mechatronics Engineering* Vol.7, No. 3, PP 159-164, 2013.
- [12] Salah Larbia, Adel El Hella, “Thermo-fluid aspect analysis of passive cooling system case using solar chimney in the south regions of Algeria”, *Energy Procedia* 36 PP. 628 – 637, 2013.
- [13] J. Mathur, et al. “ Summer-performance of inclined roof solar chimney for natural ventilation”, *Energy and Building* 38, PP. 1156-1163, 2006.
- [14] B. Belfugais, S. Larbi, “Passive Ventilation System Analysis using Solar Chimney in South of Algeria” *World Academy of Science, Engineering and Technology* Vol. 58, PP. 26-30, 2011.
- [15] C. Seytier, et al., “Combined Convective-Radiative Thermal Analysis of an Inclined Rooftop Solar Chimney” *Journal of Solar Energy Engineering*, Vol. 135 Feb. , 2013.

## دراسة عملية لاستخدام المدخنة الشمسية السلبية في التبريد التبخيري مع مادة ثنائية الطور ومصفوفة رغوة النحاس كخزان حراري

طالب كشاش مرتضى\* حسين مجيد صالح\*\* علي داود سلمان\*\*\*

\*قسم الهندسة الميكانيكية / الجامعة التكنولوجية

\*\*،\*\*\*، قسم الهندسة الكهر وميكانيكية / الجامعة التكنولوجية

\*البريد الإلكتروني: talib\_km@yahoo.com

\*البريد الإلكتروني: hussein\_maj@yahoo.com

\*\*،\*\*\*، البريد الإلكتروني: aligaphory@yahoo.com

### الخلاصة

خلال هذه الدراسة العملية، تم بناء غرفة اختبار معزولة بحجم (2\*1.5\*1.5) متر لكل من الطول والعرض وارتفاع الغرفة المبنية في مدينة بغداد. بينما صمم كلا المداخل الشمسية ضمن نسبة طول الى عرض الفجوة الهوائية بمقدار اكبر من القيمة الحرجة 12. جهزت غرفة الاختبار بعدة أنواع من المجمعات الشمسية، فهناك المدخنة العمودية الثابتة ذات الخزان الحراري المسطح والمدهون بدهان اسود غير لامع ومغلقة بسطح نفاذ للضوء وعازل حراري، وهناك المدخنة المائلة بزاوية 45 درجة والموصولة بالتوالي مع المدخنة الثابتة لزيادة ارتفاع المدخنة الكلي وتحسين توليد قوة الطفو، في هذه المدخنة ثلاثة خزانات حرارية على طول المدخنة مع وجود فجوتي هواء على طرفي المجمع لجريان الهواء خلالهما من خلال توليد قوة الطفو اللازمة عن طريق زيادة انتقال الحرارة الى الهواء مع تأمين منع حدوث جريان هواء خلفي. كما تم زراعة مجموعة من الانابيب الزجاجية المزودة والمفرغة من الهواء والتي في داخل كل واحد منها انبوب حراري وبدون حشوة (ثرموسايفون) حيث توصل هذه الانابيب المائلة بزاوية 45° الى النصف السفلي من الخزان الحراري للمدخنة الشمسية العمودية الثابتة. تم خزن حرارة الإشعاع الشمسي في المدخنة الشمسية باستخدام خزانات معدنية مغلونة تحتوي على مواد متغيرة الطور لها قابلية على خزن الحرارة ومدعمة برغوة معدنية لتحسين التوصيلية الحرارية لمادة الخزن. تستخدم الحرارة المخزونة لتوليد قوة الطفو ومن ثم حث الهواء خلال المدخنة الشمسية وعمل تخلل ضغط داخل الغرفة، للسماح للهواء الخارجي النقي بالدخول عبر فتحات تحتوي على حشوة سليلوزية لها القابلية على امتصاص الماء، وبمرور الهواء فوق سطح الحشوة المبتلة مما يؤدي إلى حدوث التبريد التبخيري. أظهرت النتائج العملية والتي تم إجرائها في بداية ومنتصف الشهر السادس، إلى إمكانية خفض درجة حرارة حيز الاختبار ضمن فترة اختبار 24 ساعة متواصلة، حيث إن أقل فرق درجة حرارة بين حيز الاختبار وظرف الهواء الخارجي كانت ما يقارب 3.5 درجة مئوية عند الساعة 20:00 مساءً وكذلك بفرق مماثل يحدث عند الساعة 03:00 صباحاً، اما أعلى فرق في درجة الحرارة بمقدار 8.5-9.2 درجة مئوية ويحدث خلال 11:00-15:00 من عمر فترة الاختبار. كما أظهرت النتائج فعالية استخدام الخزن الحراري الشمسي، لفترة ما بعد المغيب مع ملاحظة انخفاض في فعالية التبريد التبخيري، بلغت مدى فعالية التبريد التبخيري 30.5-37.5 ضمن جريان الهواء الطبيعي، اما تهوية الحيز فكان بمعدل (6.187-3.8) خلال الساعة ضمن معامل تدفق خلال المنظومة 0.371، واكبر معدل تدفق كتلي للهواء فكان بمقدار (36.651 kg.hr<sup>-1</sup>).